J|A|C|S ARTICLES

Published on Web 12/10/2009

Vesicle Budding Induced by a Pore-Forming Peptide

Yan Yu,[†] Julie A. Vroman,[†] Sung Chul Bae,[†] and Steve Granick*[,‡,§]

Departments of Materials Science and Engineering, Chemistry, and Physics, University of Illinois, Urbana, Illinois 61801

Received July 15, 2009; E-mail: sgranick@illinois.edu

Abstract: We describe, in a system whose uniqueness is that the presence of pores allows the volume to vary as budding proceeds, how phase separation on the surface of spheres extrudes material in the process called "budding". The system is giant phospholipid vesicles (GUVs) containing phase-separated regions of DOPC (soft, liquid) and DPPC (stiff, gel), with cholesterol and without it. Budding is triggered by adding the cationic pore-forming peptide, melittin. Without cholesterol, fluorescence experiments show that melittin selectively binds to the liquid domains, inducing them to form mainly exocytotic monodisperse smaller vesicle buds of this same material, causing the parent GUV to shrink. The effect of cholesterol is to produce just a few large buds following domain coalescence, rather than numerous smaller monodisperse ones. Line tension is experimentally shown to be essential for budding in this multicomponent membrane.

Introduction

The formation of vesicles by budding from cell membranes is essential to a variety of biological functions. Small vesicles are extruded from membranes to transport cargo from one compartment to another. Notable examples of this interplay between proteins and lipid membranes[1] include exocytosis of enveloped viruses,[2] transport in the Golgi apparatus and endoplasmic reticulum,[3] and signaling in neuron synapses.[4] However, complexities of the living cell render it problematic to study in vivo the mechanisms underlying protein-induced membrane budding. It is known in principle that some of the underlying mechanisms involve protein-specific factors and that others involve generic factors such as the intrinsic curvature and bending stiffness of membranes themselves,[5] but how to assess the relative importance of these contributions in specific physical situations is not understood generically.

Giant unilamellar vesicles (GUVs), with size and lipid composition similar to that in cells, have been widely used as an attractive experimental alternative to living systems. Moreover, GUVs containing different types of lipids can experience lipid phase separation in their membranes, in this respect resembling cell membranes with lipid rafts. Previous work by others has investigated how, in single-component GUVs, various proteins induce budding. It has been proposed that proteins generate membrane curvature either by embedding small amphiphilic domains into the membrane matrix or by imposing their intrinsic curvature as a scaffold.[1] An amphiphilic helix is often involved, and this contributes to the generation of curvature. It is established[6] that the insertion of an amphiphilic structure into a membrane plays an important role in membrane budding, despite protein diversity, but these in vitro studies were limited to single-component membranes.

This study concerns multicomponent membranes instead. In contrast to the extensive studies on single-component membranes,[7] experimental studies to explore the in vitro budding of heterogeneous membranes are at an early stage. Osmotic stress,[8] addition of detergent,[9] and interior phase separation[10] can induce budding of lipid rafts, and theories proposing other mechanisms have been suggested.[11] In approaching these issues experimentally, a limitation of earlier experiments was the volume constraint in a parent vesicle, which is another way of saying that the membrane prevents fluid from passing from inside to outside of the vesicles rapidly; other things equal, this should inhibit budding and further scission of buds.[12] Here, by employing a pore-forming peptide that allows exchange of the

[†] Department of Materials Science and Engineering.
[‡] Department of Chemistry.
[§] Department of Physics.

(1) Zimmerberg, J.; Kozlov, M. M. *Nature Rev. Mol. Cell. Biol.* **2006**, *7*, 9.
(2) Brügger, B.; Glass, B.; Haberkant, P.; Leibrecht, I.; Wieland, F. T.; Kräusslich, H. G. *Proc. Natl. Acad. Sci. U.S.A.* **2006**, *103*, 2641.
(3) Glick, B. S.; Malhotra, V. *Cell* **1998**, *95*, 883.
(4) Valtorta, F.; Meldolesi, J.; Fesce, R. *Trends Cell Biol.* **2001**, *11*, 404.
(5) (a) Phillips, R.; Ursell, T.; Wiggins, P.; Sens, P. *Nature* **2009**, *459*, 379. (b) Sens, P.; Ludger, J.; Bassereau, P. *Curr. Opin. Cell Biol.* **2008**, *20*, 476. (c) McMahon, H. T.; Gallop, J. L. *Nature* **2005**, *438*, 590.
(6) (a) Lee, M. C. S.; Schekman, R. *Science* **2004**, *303*, 479. (b) Lee, M. C. S.; Orci, L.; Hamamoto, S.; Futai, E.; Ravazzola, M.; Schekman, R. *Cell* **2005**, *122*, 605.
(7) (a) Tamba, Y.; Ohba, S.; Kubota, M.; Yoshioka, H.; Yoshioka, H.; Yamazaki, M. *Biophys. J.* **2007**, *92*, 3178. (b) Roux, A.; Cappello, G.; Cartaud, J.; Prost, J.; Goud, B.; Bassereau, P. *Proc. Natl. Acad, Sci. U.S.A* **2002**, *99*, 5394. (c) Domanov, Y. A.; Kinnunen, P. K. J. *Biophys. J.* **2006**, *91*, 4427.
(8) Yanagisawa, M.; Imai, M.; Taniguchi, T. *Phys. Rev. Lett.* **2008**, *100*, 148102.
(9) (a) Hamada, T.; Miura, Y.; Ishii, K.; Araki, S.; Yoshikawa, K.; Vestergaard, M.; Takagi, M. *J. Phys. Chem. B* **2007**, *111*, 10853. (b) Staneva, G.; Seigneuret, M.; Koumanov, K.; Trugnan, G.; Angelova, M. I. *Chem. Phys. Lipids* **2005**, *136*, 55.
(10) (a) Long, M. S.; Jones, C. D.; Helfrich, M. R.; Mangeney-Slavin, L. K.; Keating, C. D. *Proc. Natl. Acad. Sci. U.S.A.* **2005**, *102*, 5920–5925. (b) Long, M. S.; Cans, A.-S.; Keating, C. D. *J. Am. Chem. Soc.* **2008**, *130*, 756–762. (c) Cans, A.-S.; Andes-Koback, M.; Keating, C. D. *J. Am. Chem. Soc.* **2008**, *130*, 7400–762.
(11) (a) Lipowsky, R.; Dimova, R. *J. Phys.: Condens. Matter* **2003**, *15*, S31. (b) Kumar, P. B. S.; Gompper, G.; Lipowsky, R. *Phys. Rev. Lett.* **2001**, *86*, 3911.

aqueous medium to outside the vesicle as the vesicle shrinks from budding, we overcome this limitation.

Two additional reasons rendered melittin, an antimicrobial peptide with 26 amino acid residues, an attractive choice. First, this amphiphilic peptide, considered to be an attractive candidate to mimic the N-terminus of HIV-1 virulence factor Nef1-25 because of their significant structural similarities,[13] is a model system in which to study lipid membrane−peptide interactions. Second, this peptide forms an α-helix when rapidly binding to a lipid membrane, as do other antimicrobial peptides. At low concentrations, it situates itself between the headgroup regions of the membrane leaflet but forms transmembrane pores when its concentration exceeds certain threshold values.[14] Previous studies focused on the pore-forming mechanisms of melittin in single-component lipid bilayers.[14,15]

Experimental Procedures

Materials. 1,2-Dioleoyl-sn-glycero-3-phosphocholine (DOPC), 1,2-dipalmitoyl-sn-glycero-3-phosphocholine (DPPC), cholesterol (purity >98%), 1,2-diphytanoyl-sn-glycero-3-phosphatidylcholine (DPhPC), 1,2-dilauroyl-sn-glycero-3-phosphocholine (DLPC), the fluorescent lipids 1,2-dioleoyl-sn-glycero-3-phosphoethanolamine-*N*-(lissamine rhodamine B sulfonyl) (DOPE-RhB), and 1,2-dipalmitoyl-sn-glycero-3-phosphoethanolamine-*N*-(lissamine rhodamine B sulfonyl) (DPPE-RhB) were purchased from Avanti Polar Lipids (Alabaster, AL). Melittin (purity >95%) was purchased from Enzo Life Sciences International (Plymouth Meeting, PA). Melittin labeled with NBD at the N-terminus (purity >98%) was synthesized by the Protein Sciences Facility at the University of Illinois (Urbana, IL).

Methods. Sample Preparation. For oriented circular dichroism (OCD) measurements, the preparation of oriented peptide−lipid multilayers followed the method described by Chen et al.[14a] Briefly, lipids and peptides at chosen ratios of peptide to lipid, *P/L*, were dissolved in a 1:1 (v/v) solvent mixture of methanol and chloroform to achieve a final lipid concentration of ∼25 mg/mL. To avoid absorption flattening and linear dichroism artifacts, an appropriate amount of the solution (10 μL or less depending on the *P/L*) was deposited to an area about 14 mm in diameter on a precleaned quartz glass surface to form a thin film sample. After the solvent evaporated, the sample was subjected to vacuum for at least 3 h to remove solvent residue and then slowly hydrated for ∼15 h at 30 °C and 97.0% relative humidity, obtained by using a saturated K_2SO_4 solution. Finally, the sample cell was assembled and sealed with vacuum grease to ensure no change of humidity during OCD measurements.

For fluorescence imaging, giant unilamellar vesicles (GUVs) were prepared using the electroformation method described by Angelova et al.[16] Vesicles were prepared in deionized water (Millipore) and grown at 2 V/mm and 5 Hz for 2 h at 60 °C. A concentration of 0.2 mol % of fluorescently labeled lipids was used for contrast between phases. After GUVs were prepared, melittin previously dissolved in deionized (DI) water was added and the solution was incubated for 2−3 min at 60 °C before being quenched to 20 °C for imaging.

For consistency with the OCD results, the peptide-to-lipid ratio (*P/L*) here is the ratio between the number of melittin *bound* to the membrane and the total number of lipids, estimated based on a partition equilibrium that holds in the regime of low melittin concentration, low enough that pores do not form: $P/L = (K_P C_P)/(1 + K_P(C_P + C_L))$, where C_P and C_L are the concentration of melittin and lipids, respectively, and K_P is the partition coefficient of melittin to DOPC lipid bilayer. Here, $K_P = 2.3 \times 10^4\ M^{-1}$ obtained by Wessman et al.[17] was used. The fraction of melittin bound to membrane was calculated to be ∼50% of the total.

OCD Measurement. OCD measurements were carried out at 25 °C using a Jasco 715 spectropolarimeter (Jasco, Tokyo, Japan), with incident light normal to the sample surface. OCD spectra were acquired between 260 and 180 nm at 0.1-nm intervals. Three repeat scans at the scan rate of 10 nm/min, 4 s response, and 1 nm bandwidth were averaged for each sample at every 45° of rotation of the sample cell to eliminate possible artifacts due to linear dichroism. The hydration equilibrium of the sample was confirmed by agreement of OCD spectra over a period of 4 h. The OCD spectra for two extreme orientations of melittin in lipid layers, parallel to the bilayers (the S state) and normal to them (the I state), were measured in DPhPC (*P/L* = 1/30) and DLPC (*P/L* = 1/30) multilayers, respectively.[14c] The background OCD spectra of pure lipid bilayers were measured separately and subtracted from the spectra of the corresponding samples with peptides. To analyze the fraction of melittin in the S or I state, each calibrated spectrum was normalized to the relative amount of melittin in its corresponding sample and fitted by a linear combination of the S and I spectra at wavelengths above 200 nm. The noise levels were high at wavelengths below 200 nm owing to the strong UV absorbance of DOPC.

Fluorescence Imaging. To visualize lipid domains in GUVs, images of the GUVs were mainly obtained using a home-built epifluorescence imaging microscope equipped with a Nd:YVO_4 laser of 532 nm excitation wavelength. Some dual-color images of GUVs and melittin-NBD were obtained using a Leika SP2 confocal microscope in the Microscopy Suite, Beckman Institute, University of Illinois (Urbana, IL). DOPE-RhB or DPPE-RhB was excited at 543 nm and imaged at 560−620 nm. Melittin−NBD was excited at 488 nm and imaged at 500−530 nm. Consecutive scanning was performed to ensure no crosstalk between two channels. To quantify the size of the vesicle buds, the fluorescence image of each bud was fitted to a two-dimensional Gaussian distribution as described previously,[18] from which the variance (σ) was obtained as a measure of bud size. Subject to the optical diffraction limit of ∼300 nm (half the peak of the fluorescence wavelength), the diameter of the buds was estimated based on a reference plot in which σ of fluorescent polystyrene nanoparticles (Invitrogen, Carlbad, CA) with known sizes was plotted versus diameter (*D*) (see Figure S1 in Supporting Information).

Results and Discussion

Melittin Orientation within Bilayers. First we establish the concentration at which melittin forms membrane-spanning pores when it adsorbs onto phase-separated lipid bilayers. The lipid bilayer was a mixture of DOPC and DPPC at a molar ratio of 1:4, a composition at which the phase-separated regions form stripe phases of regular thickness.[19,20] DOPC with phase transition temperature (T_m) of −20 °C is in the

(12) Lipowsky, R.; Brinkmann, M.; Dimova, R.; Haluska, C.; Kierfeld, J.; Shillcock, J. *J. Phys.: Condens. Matter* **2005**, *17*, S2885.
(13) Barnham, K. J.; Monks, S. A.; Hinds, M. G.; Azad, A. A.; Norton, R. S. *Biochemistry* **1997**, *36*, 5970.
(14) (a) Hristova, K.; Dempsey, C. E.; White, S. H. *Biophys. J.* **2001**, *80*, 801. (b) Yang, L.; Harroun, T. A.; Weiss, T. M.; Ding, L.; Huang, H. W. *Biophys. J.* **2001**, *81*, 1475. (c) Lee, M.-T.; Hung, W.-C.; Chen, F.-Y.; Huang, H. W. *Proc. Natl. Acad. Sci. U.S.A.* **2008**, *105*, 5087. (d) van den Bogaart, G.; Guzmán, J. V.; Mika, J. T.; Poolman, B. *J. Biol. Chem.* **2008**, *283*, 33854.
(15) (a) Kriech, M. A.; Conboy, J. C. *J. Am. Soc. Chem.* **2003**, *125*, 1148. (b) Sharon, M.; Oren, Z.; Shai, Y.; Anglister, J. *Biochemistry* **1999**, *38*, 15305. (c) Chen, X.; Wang, J.; Boughton, A. P.; Kristalyn, C. B.; Chen, Z. *J. Am. Soc. Chem.* **2007**, *129*, 1420.
(16) Angelova, M. I.; Soléau, S.; Méléard, Ph.; Faucon, F.; Bothorel, P. *Prog. Colloid Polym. Sci.* **1992**, *89*, 127.
(17) Wessman, P.; Strömstedt, A. A.; Malmsten, M.; Edwards, K. *Biophys. J.* **2008**, *95*, 4324.
(18) Anthony, S. M.; Granick, S. *Langmuir* **2009**, *25*, 8152.
(19) Korlach, J.; Schwille, P.; Webb, W. W.; Feigenson, G. W. *Proc. Natl. Acad. Sci. U.S.A.* **1999**, *96*, 8461.
(20) Li, L.; Cheng, J.-X. *Biochemistry* **2006**, *45*, 11819.

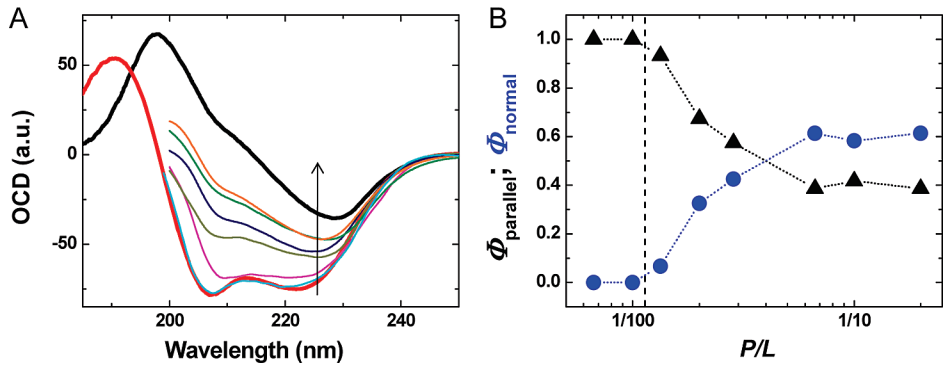

Figure 1. Melittin orientation in bilayers. (A) Oriented circular dichroism (OCD) of melittin embedded in DOPC/DPPC (1/4) multilayers at $P/L = 1/100$, 1/75, 1/50, 1/35, 1/10, and 1/5 (from bottom to top, indicated by the arrow). Here the solid lines show the limits of complete parallel and perpendicular orientation, the S and I states, respectively. Each intermediate spectrum was fitted by a linear combination of S and I to obtain the fraction of melittin in these two states. (B) The fractions of melittin oriented parallel ($F_{parallel}$, triangles) or normal (F_{normal}, circles) to the multilayers at 25 °C, plotted against the peptide/lipid ratio, *P/L*. The vertical dashed line indicates onset of pore formation.

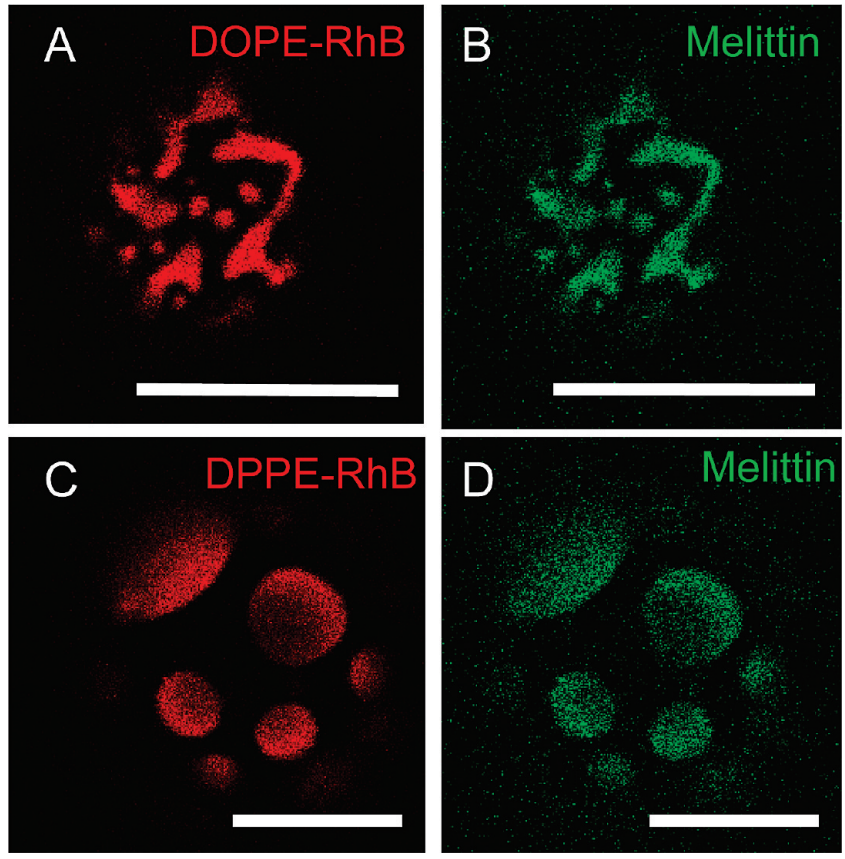

Figure 2. Confocal fluorescence images focused at the top of the GUV showing that melittin binds selectively to DOPC-rich (liquid-phase) domains in phase-separated GUVs containing DOPC, DPPC, and cholesterol. Melittin covalently labeled with NBD at the N-terminus was added at peptide/lipid ratio $P/L = 1/100$. Panels A and B refer to GUVs composed of DOPC/DPPC = 1/4, which at 20 °C exhibit liquid/gel phase coexistence, the liquid phase enriched in DOPC and gel phase enriched in DPPC. Panels C and D refer to GUVs composed of DOPC/DPPC/chol = 1/3/1. Both cases contain dye (0.2 mol % DOPE-RhB and DPPE-RhB, respectively) that partitions preferentially into the DOPC phase. In these two-color confocal images, the (red) lipid and the (green) melittin coincide in position. Scale bars: 10 μm.

liquid phase at room temperature while DPPC ($T_m = 41$ °C) is in the gel phase; the mixture exhibits liquid/gel phase coexistence, the liquid phase enriched in DOPC and the gel phase enriched in DPPC.

In the circular dichroism experiments illustrated in Figure 1A, the two thick lines indicate the S and I state spectra when all melittins are oriented parallel or normal to the multiple bilayers, and the thin lines represent some of the normalized OCD spectra of melittin in the DOPC/DPPC bilayers at various peptide/lipid (*P/L*) ratios. The fraction of melittin in the S and I states, deduced as described in Experimental Procedures, are shown in Figure 1B. It is clear that melittin lies completely parallel to the bilayers at low concentrations. Above $P/L^* \approx 1/88$, denoted by the vertical dashed line in Panel B and determined according to the method described by Lee et al.,[14c] some melittin helices penetrate into the bilayers and pores begin to form. As the melittin concentration increases, the fraction of melittin oriented normal to the bilayers increases until at elevated

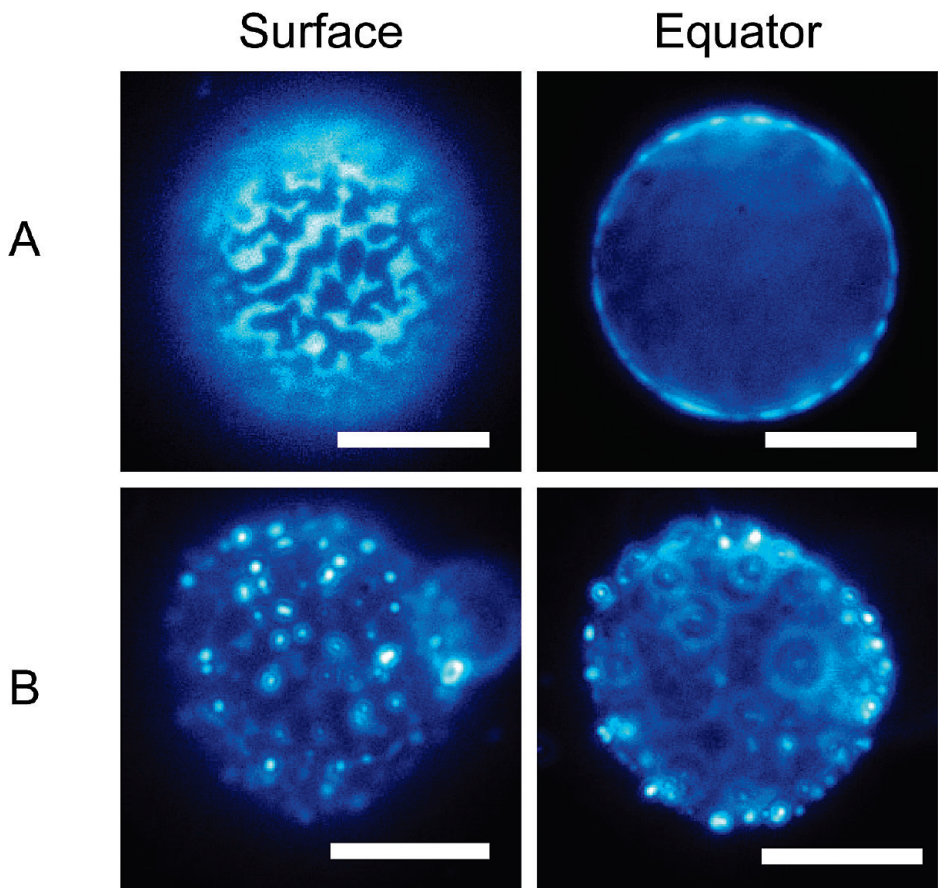

Figure 3. Epifluorescence images of giant unilamellar vesicles composed of DOPC/DPPC = 1/4 with 0.2 mol % DOPE-RhB which segregates into liquid (DOPC-rich) domains. (A) In the absence of melittin, the stripe domains in a typical GUV. (B) In the presence of melittin, at peptide/lipid ratio $P/L = 1/10$, budding ensues. In the left and right columns, the "surface" and "equator" columns, respectively, the confocal image was focused at the top and midway through the GUV. Scale bars: 10 μm.

concentrations, $P/L > 1/15$, the fraction of melittin in the two orientations appears to remain constant.

Melittin Spatial Selectivity. With the aim to study whether melittin binds preferentially to either phase-separated domain, we prepared giant unilamellar vesicles (GUVs) with the same lipid composition. For comparison, we also prepared mixtures including cholesterol at the molar ratio DOPC:DPPC:chol = 1:3:1, a composition chosen with guidance from a well-known phase diagram,[21] because it was close to the composition of DOPC:DPPC = 1:4 and the lipid phase separation forms relatively monodisperse circular domains, enabling observation of possible morphological changes. To image simultaneously the lipid domains and the location of melittin, DOPE-RhB (0.2 mol %) was included to preferentially label the liquid domains,[20] and melittin, labeled with a small dye 6-(*N*-(7-nitrobenz-2-oxa-1,3-diazol-4-yl)amino)hexanoate (NBD) at its N-terminus, was added at $P/L = 1/200$. The melittin concentration was chosen to be well below P/L^* so that pores were not present. Labeling has been shown to affect neither the binding nor the pore-forming properties of melittin.[22]

Dual-color confocal fluorescence images of a GUV membrane surface (Figures 2A and Figure 2B) show that melittin is nearly exclusively located in the liquid phase enriched in DOPC. A second significant observation is that the fluorescence intensity from the NBD labels suggests no accumulation of melittin at the domain boundaries.

In the presence of cholesterol, DOPC/DPPC/chol GUVs exhibit liquid disordered (l_d)/liquid ordered (l_o) phase coexistence, where the structure of the l_d and l_o domains differs from liquid and gel domains owing to the participation of cholesterol in both phases. DPPE-RhB was used to selectively label l_d domains.[21] Figure 2C and 2D show that melittin continues to bind selectively to DOPC-rich domains, also in the presence of cholesterol.

This spatial preference of melittin may reflect the relative compressibility of the phase-separated domains. Indeed, pore formation by melittin has been suggested to depend on lipid composition and physical properties of the membrane, such as spontaneous curvature and the compressibility modulus.[23] The compressibility modulus of DPPC in the gel phase is ~800 mN/m,[24] while for DOPC in the liquid state it is ~240 mN/m.[25] Therefore, liquid domains enriched in DOPC can more easily accommodate the surface expansion associated with melittin binding.

(21) Veatch, S. L.; Keller, S. L. *Biophys. J.* **2003**, *85*, 3074.
(22) Raghuraman, H.; Chattopadhyay, A. *Biophys. J.* **2007**, *92*, 1271.
(23) (a) van den Bogaart, G.; Mika, J. T.; Krasnikov, V.; Poolman, B. *Biophys. J.* **2007**, *93*, 154. (b) Allende, D.; Simon, S. A.; McIntosh, T. J. *Biophys. J.* **2005**, *88*, 1828.
(24) Feller, S. E.; Pastor, R. W. *J. Chem. Phys.* **1999**, *111*, 1281.
(25) Rawicz, W.; Olbrich, K. C.; McIntosh, T.; Needham, D.; Evans, E. *Biophys. J.* **2000**, *79*, 328.

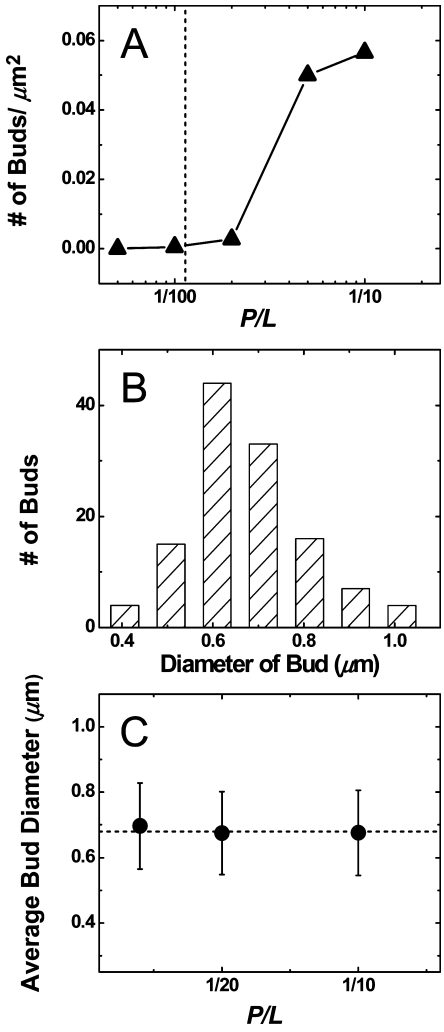

Figure 4. Quantification of melittin-induced budding. (A) The number of buds per square micrometer is plotted against *P/L*. The vertical dash line indicates onset of pore formation. (B) Distribution of bud diameter at $P/L = 1/20$, obtained from a random sample of 150 spheres from 10 GUVs. (C) The average bud diameter plotted against the peptide/lipid ratio, *P/L*. Error bars are standard deviations of the size distributions.

Lipid Composition of Buds. Liquid domains labeled by DOPE-RhB exhibit a stripe-like morphology in the absence of melittin (Figure 3A). However, with melittin at $P/L = 1/10$, a concentration after pore formation, many small fluorescent spheres formed on the outer leaflet of the liquid domains, giving the appearance of liposome extrudates, and some of them became detached (Figure 3B). The majority of the buds were generated via an exocytic process, toward the outside of the GUVs, though ones toward the inside were also observed occasionally (see Figure S2 in Supporting Information.). Meanwhile, the GUVs shrank, reflecting loss of volume owing to this budding. The observation is a phenomenon different from the phase-separated vesicle membranes decorated with domain caps,[26] in which further capping is suppressed by lateral tension on the membrane because of the constraint of maintaining constant volume. In the present case, in the presence of melittin pores, the domain caps are allowed to reshape into buds which eventually detach.

We estimate the lipid composition in these small spheres to be approximately the same as in liquid domains of the mother GUV, based on two observations: (i) Surface area of the fluorescently labeled domains decreased correspondingly with budding formation; (ii) the fluorescence intensity observed at the center of the smaller spheres is approximately twice that of liquid domains in the absence of melittin. As for small vesicles, the optical image is a two-dimensional projection of two lipid bilayers, whereas for the parent GUV, the vesicle is so large that the optical image contains a fluorescent signal from only one bilayer. The factor of 2 in fluorescence intensity difference suggests the same lipid composition in both systems. Melittin was found to be uniformly distributed in the vesicle buds and the liquid domains in the mother GUV membrane, judged from its fluorescence intensity at different locations in confocal fluorescence images.

Size and Abundance of Buds. In Figure 4A, the average number of buds per surface area on the GUV membrane is plotted against *P/L* and the onset of pore formation is indicated by a vertical dashed line. No budding was observed before pores began to form. Pore abundance increased sharply in the regime $P/L > 1/50$.

The diameter of individual vesicle buds at different *P/L* ratios was quantified by analyzing the images of 10 GUVs using 2-D Gaussian fitting of the fluorescence intensities and meticulous calibration, yielding a random sample of 150 spheres. As illustrated in Figure 4B, the histogram of bud diameters at $P/L = 1/20$ has a narrow distribution, 0.4 to 1 μm. Of course, quantification of the lower range is limited by the optical diffraction limit, $\sim$300 nm under the experimental condition. Similar sizes, all narrow in distribution, were also observed for $P/L = 1/50$ and 1/10 (see Figure S3 of Supporting Information). Figure 4C shows that the mean diameter of vesicle buds remains the same regardless of melittin concentration. Despite the diffraction limitation, it is evident that budded vesicles have an intrinsic curvature independent of melittin concentration in the parent GUV, which implies that neither spontaneous curvature nor area difference caused by melittin binding determines the size of the vesicle buds.

Energetically, line tension favors budding and bending rigidity opposes it. Bearing in mind that binding of melittin to lipid bilayers at low concentrations has been suggested to cause membrane thinning,[14c] it is reasonable that in this system also, melittin adsorption expands the lipid headgroup area, causing the bilayer thickness to decrease, and that the thinning effect is roughly proportional to *P/L*. The unbalanced expansion of the two leaflets due to asymmetric binding of melittin can produce nonzero spontaneous curvature in the DOPC-rich liquid domains, which has been suggested by simulation[11b] to be the driving force for budding in a two-component membrane. Meanwhile, interfacially adsorbed amphiphilic rod inclusions on lipid membranes have been suggested by simulations to induce different spontaneous curvatures dependent on their penetration depth.[27] Melittin penetrates into the DOPC bilayer at a distance of $\sim$18 Å from the center of the bilayer whose thickness is $\sim$49 Å,[14a] a relatively shallow insertion expected to cause a positive curvature (membrane bulging toward the peptide), which is consistent with our observation of the mainly exocytotic budding formation. The possible effect of osmotic

(26) (a) Baumgart, T.; Hess, S. T.; Webb, W. W. *Nature* **2003**, *425*, 821. (b) Veatch, S. L.; Keller, S. L. *Phys. Rev. Lett.* **2002**, *89*, 268101.

(27) (a) Campelo, F.; McMahon, H. T.; Kozlov, M. M. *Biophys. J.* **2008**, *95*, 2325. (b) Zemel, A.; Ben-Shaul, A.; May, S. *J. Phys. Chem. B* **2008**, *112*, 6988.

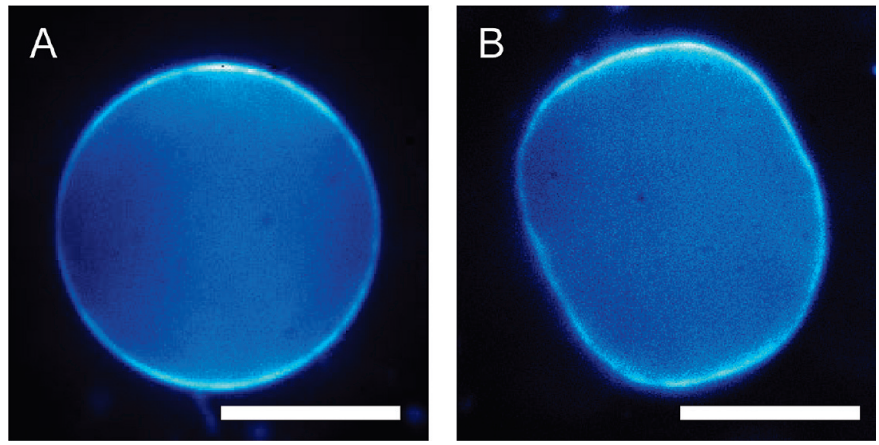

Figure 5. Comparison of the shape of single-component DOPC giant unilamellar vesicles vesicles, containing 0.2 mol % DOPE-RhB, in the absence of melittin (panel A) and in the presence of melittin at $P/L = 1/20$ (panel B). The prolate shape in panel B fluctuates in time for up to 3−4 h. Scale bars: 10 μm.

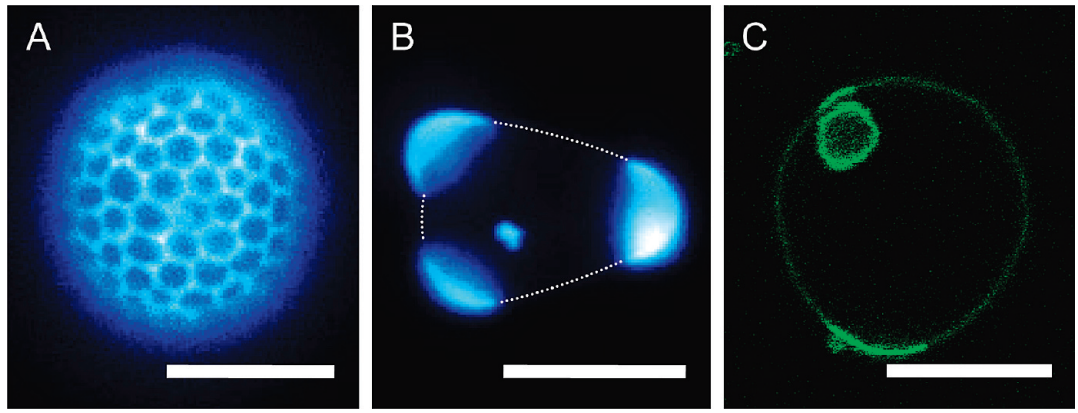

Figure 6. Fluorescence images of phase coexistence in the absence of melittin (panel A) and with melittin at $P/L = 1/50$ (panel B and C), for GUVs composed of DOPC/DPPC/cholesterol = 1/3/1 with 0.2 mol % DPPE-RhB to selectively label the l_d DOPC-rich domains. Without melittin, a hexagonal microstructure forms in which a continuous liquid disordered (l_d) phase surrounds patches of liquid ordered (l_o) domains. The hexagonal microstructure is lost, and domains coalesced and budded out after 1−2 h, upon adding melittin. Panel A and B are epifluorescence images, and Panel C is a confocal fluorescence image. Dotted lines in Panel B outline the rim of the GUV, as a guide to the eye. Scale bars: 10 μm.

stress is excluded because of the pore formation and the significantly low concentration of melittin (0.1−2 μM) which is orders of magnitude lower than the concentration of salt (a few mM) reported to induce vesicle budding.[9a]

Line Tension. As shown in Figure 5, upon adding melittin at $P/L = 1/20$, the shape of single-component DOPC GUVs is no longer spherical; instead it is a prolate "potato" shape, and this shape fluctuates in time, which is consistent with the increased spontaneous curvature just discussed. However, no budding was observed even at the highest melittin concentrations, except in the presence of phase-separated lipids.

To explore experimentally the role of line tension and bending rigidity, a few experiments were performed in the presence of cholesterol, which reduces line tension but increases membrane bending rigidity.[18,28] Figure 6A shows fluorescence images in the absence of melittin for GUVs of DOPC/DPPC/chol at a molar ratio of 1:3:1; one observes coexistence of mostly discontinuous l_o domains surrounded by continuous l_d domains. Figure 6B shows that within minutes after adding melittin, coalescence of domains was observed starting at $P/L = 1/100$ and prominently so at $P/L > 1/50$. After 1−2 h, the large l_d patches eventually budded out as a whole, leaving GUVs with homogeneous but faint fluorescence. In addition to the effects of reduced line tension and increased bending rigidity, cholesterol is known to reduce the affinity of melittin to DOPC membranes.[29] This could result in a less prominent spontaneous curvature influence to promote budding. These observations in the presence of cholesterol have some potential relevance to the fact that the membranes of living cells have been proposed to adapt the cholesterol composition in lipid rafts to accommodate various cellular functions,[1,30] but no quantitative connection is proposed at this time.

The complexity of these multicomponent systems appears to preclude a direct comparison to theories of membrane physics,[5,10] so at this time we aim to generalize from experiment. It is clear that the dynamic pathway of budding changed by adding cholesterol, but for now we leave it as a parenthetical observation to the main point of this study, which is the need of line tension for budding in a phase-separated morphology and the effectiveness of releasing the volume constraint to permit

(28) Bennett, W. F. D.; MacCallum, J. L.; Tieleman, D. P. *J. Am. Chem. Soc.* **2009**, *131*, 1972.

(29) Wessman, P.; Strömstedt, A. A.; Malmsten, M.; Edwards, K. *Biophys. J.* **2008**, *95*, 4324.

(30) Roux, A.; Cuvelier, D.; Nassoy, P.; Prost, J.; Bassereau, P.; Goud, B. *EMBO J.* **2005**, *24*, 1537.

budding, and the capacity demonstrated here to produce monodisperse buds simply by adding amphipathic peptide.

Acknowledgment. We are indebted to Pierre Sens and Patricia Bassereau for helpful discussion and to Scott E. Denmark for use of the CD instrument in his laboratory. This work was supported by the U.S. Department of Energy, Division of Materials Science, under Award No. DEFG02-02ER46019. S.C.B. acknowledges NSF-DMR-0117792 and NSF-DMR-0907018. J.A.V. acknowledges NSF-CMS-055820 and NSF-CBET-08-53737.

Supporting Information Available: Additional information as noted in the text. This material is available free of charge via the Internet at http://pubs.acs.org.

JA9059014